PRODUCTION AND PROPERTIES OF LOW-DENSITY ALKALI-ACTIVATED COMPOSITES BY INCORPORATION OF EXPANDED POLYSTYRENE (EPS)

Adriano Galvão Souza Azevedo[1]*, Carolina Torga Lombardi[3], Luis Fernando Tonholo Domingos[2], Kurt Strecker[3]

1: University of São Paulo (USP). Department of Biosystems Engineering (ZEB). Pirassununga, São Paulo, Brazil.

2: Department of Natural Sciences, Federal University of São João del Rei, 36301-160, São João del Rei, Minas Gerais, Brazil

3: Department of Mechanical Engineering and Production, Federal University of São João del Rei, 36307-352, São João del Rei, Minas Gerais, Brazil

**e-mail: adrianogalvao@usp.com*

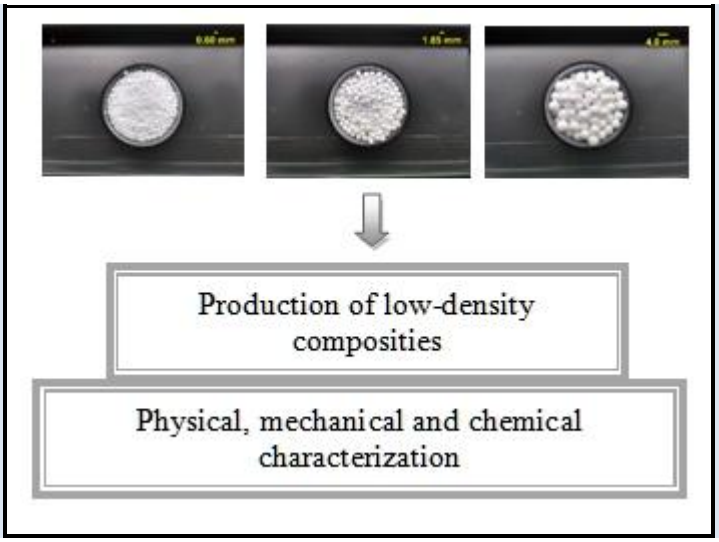

ABSTRACT

The increasing consumption of Portland cement raised concerns about the large amount of CO_2 generated during its production, Alkali-Activated Materials (AAM) being an alternative for its replacement in some applications. This research investigated the production of lightweight Alkali-Activated Composites (AAC), based on metakaolin and expanded polystyrene (EPS) as an agglomerate. The effects of the amount and size of EPS incorporated in the matrix (18, 35 and 53vol.-% and varied average sizes of 0.85, 2.16, and 6.00 mm) were evaluated. Increasing amounts of EPS reduced strength, from 42 MPa to 25 or 14 MPa for 18 or 53vol.-% of beads of size 0.85 mm. Strength decrease is more pronounced for larger EPS beads, i.e. to 12.2 and 1.5 MPa when 18 or 53vol.-% EPS beads with an average diameter of 6.0 mm were added. However, composites with a density as low as 0.8 to 1.2 g/cm^3 were produced with strength varying between 15 and 25 MPa, demonstrating their potential as construction materials for non-structural applications.

Keywords: *Alkali-activated materials, low-weight composites, expanded polystyrene, compressive strength.*

Recibido: 22-11-2021 ; **Revisado:** 12-01-2022

Aceptado: 13-04-2022 ; **Publicado:** 19-07-2022

Doi: 10.5281/zenodo.7213553

pISSN: 0255-6952 | eISSN: 2244-7113

Rev. LatinAm. Metal. Mat. 2022; **42** (1): 3-19

PRODUCTION AND PROPERTIES OF LOW-DENSITY ALKALI-ACTIVATED COMPOSITES BY INCORPORATION OF EXPANDED POLYSTYRENE (EPS)

RESUMO

O aumento do consumo de cimento Portland levantou preocupações sobre a grande quantidade de CO_2 gerado durante sua produção, sendo os materiais álcali-ativados (AAM) uma alternativa para sua substituição em algumas aplicações. Esta pesquisa investigou a produção de Compósitos Ativados por Álcalis leves (AAC), à base de metacaulim e poliestireno expandido (EPS) como aglomerado. Foram avaliados os efeitos da quantidade e tamanho do EPS incorporado na matriz (18, 35 e 53 vol .-% e tamanhos médios variados de 0,85, 2,16 e 6,00 mm). Quantidades crescentes de EPS reduziram a resistência, de 42 MPa para 25 ou 14 MPa para 18 ou 53 vol .-% de grânulos de tamanho 0,85 mm. A diminuição da resistência é mais pronunciada para grânulos de EPS maiores, ou seja, para 12,2 e 1,5 MPa quando 18 ou 53 vol .-% grânulos de EPS com um diâmetro médio de 6,0 mm foram adicionados. Porém, compósitos com densidade tão baixa quanto 0,8 a 1,2 g/cm^3 foram produzidos com resistência variando entre 15 e 25 MPa, demonstrando seu potencial como materiais de construção para aplicações não estruturais.

Palavras-chave: *Materiais álcali-ativados, compósitos de baixo peso, poliestireno expandido, resistência à compressão*

1. INTRODUCTION

The civil engineering construction industry is a sector that increasingly encompasses new areas, both in the deployment and production phases. Ordinary Portland cement (OPC) is the main construction material worldwide and has been used for many years, mainly due to its good physical, chemical, and mechanical properties, besides its low cost. However, due to its negative environmental impact by large amounts of the greenhouse gas CO_2 released during its production [1,2], growing demand for the development of new materials with the potential of replacing OPC in civil construction exists. A new category of inorganic binding materials, the so-called alkali-activated materials AAM (geopolymers), has been developed and studied by researchers all over the world, presenting mechanical properties comparable to OPC, while exhibiting lower density, and, therefore, potential to substitute OPC in certain applications [3-5]. As presented by Palomo et.al. (2021), there is a need to create alternative inorganic binders to traditional Portland cement as a way to reduce the environmental impacts generated by the construction industry. The authors present the alkaline activation technology as an alternative to traditional binders, making it possible to adapt OPC industries to produce AAM and reducing the amount of greenhouse gases released annually by the construction sector [6].

AAM is rich in aluminosilicates, presenting structures that vary according to its chemical composition, as shown in Table 1 [7-9]. These materials exhibit high mechanical strength, rapid strength gain in short periods, resistance to acid and sulfate attacks, resistance to thawing cycles, and structural stability when subjected to high temperatures, among others [5, 7]. On the other hand, the use of highly alkaline solutions makes it difficult to apply alkali activated materials. The workability of the pastes is influenced due to the chemical nature of the activating solutions. The use of AAM in the production of composites is still a point to be further researched so that the alkaline environment does not degrade the materials used as reinforcement, for example: production of fiber cements with vegetable fibers [10-11].

Table 1. Basic monomer units of formation of AAM.

Monomer	*Si/Al ratio*
Poly(sialate) (-Si-O-A_l-O-)	1:1
Poly(sialate-siloxy) (-Si-O-A_l-O-Si-O-)	2:1
Poly(sialate-disiloxy) (-Si-O-A_l-O-Si-O-Si-O-)	3:1

Since the late seventies in the twentieth century, alkali-activated materials were already considered as a potential material to replace traditional structural materials due to its excellent properties [3]. AAM, although considered being innovative materials, has been used in concretes and mortars since the time of construction of the Egyptian pyramids [12].

EPS is a rigid cellular plastic material, produced by the polymerization of styrene in water with further expansion. The final product consists of beads up to 3 mm in diameters, which then are expanded. In the expansion process, these beads are subjected to an increase of up to 50 times their initial size by steam and can be melted and shaped in various forms. After expansion, the beads consist of up to 98% air and only 2% polystyrene [13-15]. Expanded Polystyrene (EPS) has numerous applications, mainly due to its specific properties such as thermal and acoustic insulation material and its extremely low specific mass. In the work of Dueramae et. al. (2021), the authors demonstrated the possibility of using EPS for the production of low-density cementitious matrix composites. The results showed that the EPS volumetric percentage is an important factor in the final properties of the composites obtained, mainly in density and mechanical strength. The authors classified the composite as lightweight controlled low strength materials [16].

In this work the production of an alkali-activated composite based on metakaolin (MK) with incorporations of expanded polystyrene, EPS, of 18, 35, and 53 vol.-%. EPS has been chosen as aggregate due to its extremely low specific mass for

the production of lightweight construction materials, similar to lightweight concrete composites.

2. MATERIALS AND METHODS

2.1 Materials

For the preparation of the alkali-activated material, metakaolin from Metacaulim do Brasil LTDA was used. The chemical composition of the metakaolin used is shown in Table 2. The chemical composition of the metakaolin used is similar to the starting material used in the synthesis of AAM in the work of Azevedo A.R.G et al (2021) [17], in which the percentage of SiO_2 and Al_2O_3 constitutes more than 90% of the material. The alkaline activator solution was prepared with sodium hydroxide p.a., Sulfal Química LTDA, purity of 98%. Furthermore, sodium silicate (Na_2SiO_3) was added to the NaOH solution. Sodium silicate was purchased from Diatom ®, code R-2252, and its composition, provided by the manufacturer, is shown in Table 3. For the preparation of the composites, expanded polystyrene (EPS) beads were used as aggregate. The EPS used was purchased in three different average diameters of 0.85, 2.16, and 6.00 mm, as presented in Figure 1. Table 4 presents the values related to the density and the diameter of the EPS beads used to produce the AAC.

Table 2. Chemical composition of the metakaolin used to produce the AAC (wt%).

SiO_2	Al_2O_3	Fe_2O_3	TiO_2	CaO	MgO	K_2O	Na_2O	SO_2	LOI
58.7	33.4	2.1	1.3	0.1	0.2	1.6	0.1	0.2	2.3

LOI = Lost in fire

Table 3. Composition and physical properties of alkali silicate (data supplied by the manufacturer).

Composition		*Total solids*	*Humidity*	*Density (g/cm^3)*	*Viscosity (cP)*
Na_2O	14.98%	48.5%	51.45%	1.58	1.35
SiO_2	33.57%				
SiO_2/Na_2O	2.40				

Table 4. Average diameter and density of the EPS beads used as the disperse phase in the AAC.

EPS Sample	*The average diameter of EPS beads(mm)*	*Density EPS beads (g/cm³)*
A	0.85	2.7×10^{-2}
B	2.16	1.49×10^{-2}
C	6.00	1.29×10^{-2}

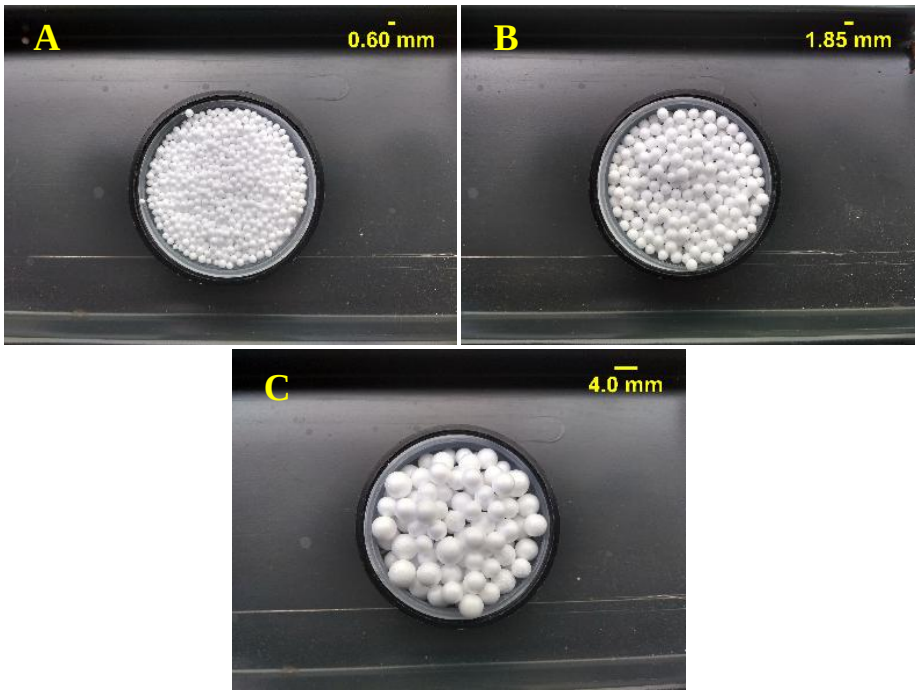

Figure 1. EPS beads: ØA = 0.85 mm; ØB = 2.16 mm and ØC = 6.00 mm.

2.2 Methods

2.2.1 Activator solution

A solution of 8 M NaOH was used for the activation of MK. The solution was prepared by dissolving sodium hydroxide in deionized water. The procedure was performed 24 hours before mixing with MK to avoid reaction modifications due to the heat released by NaOH in H_2O. 50% by weight of 8M solution was replaced with sodium silicate (Na_2SiO_3).

2.2.2 Fabrication of the alkali-activated composites

The AAM was prepared by mixing MK with the activator solution at room temperature at a ratio of 0.9 MK/(NaOH + Na_2SiO_3). The addition of further water (water/MK = 5%) was necessary to ensure the workability of the produced paste. The EPS beads of different diameters were then added to the mixtures in volumetric percentages of 18, 35, and 53%, and mixed manually. The pastes were poured into plastic molds of 60 mm height and 30 mm diameter. The filling was done gradually in three steps; at each step, the specimens were vibrated for about 20 seconds to remove entrapped air bubbles. After filling the molds, the samples were sealed with plastic film for 24 hours to prevent early loss of water. After 1 day, the plastic film was removed and the samples were cured at 60°C for 24 hours. The mechanical properties and physical characterization of the specimens were conducted after further curing for 28 days at room temperature (± 25°C). The compression tests were carried out without stopping the reactions of the produced systems.

The experimental methodology has been based on the statistical approach of experimental planning and analysis by Montgomery [18], following the itinerary suggested by Werkema and Aguiar [19].

The influence of the volumetric percentage of EPS incorporated in the alkali-activated matrix was investigated in three levels of 18, 35, and 53%, and that of the diameter was also analyzed in three levels of 0.85, 2.16, and 6.00 mm. The factors kept constant in the experiment were the proportion (in mass) between the compound solution and MK equal to 0.9 ((MK/sol. NaOH + sol. Na_2SiO_3) = 0.9), the ratio between Na_2SiO_3 and NaOH solutions was equal to 1, the molarity of the NaOH activating solution 8M, the mass percentage of additional water concerning MK equal to 5% to improve workability, an initial curing temperature (first 24 hours) of 60 °C and a curing time of 28 days (room temperature ± 25°C).

For the analysis of the response variables, a complete

factorial design was adopted. The experiments were carried out on all combinations of possible factor levels. The factorial design of type 3^2 provides 9 different experimental conditions (C1 to C9), as shown in Table 5. A reference sample was also produced to compare the results of the composites with the alkali-activated matrix, designated as Ref.

Table 5. Compositions used in the preparation of AAC.

	MK (% vol.)	*EPS (% vol.)*	*Average EPS diameter (mm)*	*MK / ($NaOH$ + Na_2SiO_3) ratio*	*Additional water (%)*
C1	82	18	0.85	0.9	5
C2	65	35	0.85	0.9	5
C3	47	53	0.85	0.9	5
C4	82	18	2.16	0.9	5
C5	65	35	2.16	0.9	5
C6	47	53	2.16	0.9	5
C7	82	18	6.00	0.9	5
C8	65	35	6.00	0.9	5
C9	47	53	6.00	0.9	5
Ref	100	--	--	0.9	5

2.2.3 Characterization of the AAC

A total of 5 specimens of each composition studied were used to determine the compressive strength. Strength was measured in uniaxial compression as described by the standard NBR – 5739 [20], using a universal testing machine, Shimadzu model AG - X plus, under a crosshead speed of 2 mm/min. The data were treated using the software Trapezium X - version 1.2.6 - Shimadzu®.

The microstructure of the composites was observed by scanning electron microscopy, Hitachi, model TM 300, with accoupled EDS, Bruker, model X-Flash, and SVE. The physical properties of the composites were obtained following the instructions of the British Standard BS EN ISO 10545-3 (1997) [21]. Infrared spectroscopy was carried out using a PerkinElmer Spectrometer, model Spectrum 1000. The analysis was done by mixing inorganic binder samples in powder form and the MK used with KBr (1:300), compacting pellets, and analyzing the sample in the range of 400 to 4000 cm^{-1} with a resolution of 4 cm^{-1} and a total of 64 scan were performed. Phase analysis was done by X-ray diffraction analysis, in a diffractometer Shimadzu model XRD 6000, using Cukα radiation (λ = 1,04059 Å) in the 2Θ range of 5 to 80°, 40 kV and 40 mA with a scan step size of 0.02. The crystal phases were identified by comparison with the ICDD, using the software HighScore Plus 3.0® (PANalytical).

3. RESULTS AND DISCUSSION

3.1 Analysis of crystalline phases (DRX)

Diffractograms referring to metakaolin and inorganic matrix after alkaline activation are shown in Figure 2. It is possible to observe in the X-ray diffractogram referring to MK, the presence of peaks corresponding to the crystalline phases of quartz (SiO_2), kaolinite ($Al_2Si_2O_5(OH)_4$), and muscovite ($KAl_2Si_3AlO_{10}(OH, F)_2$). It is also possible to observe the halo present between ~18 and 38° (2Θ), which is characteristic of material with short-range atomic ordering (amorphous material). Similar results were obtained in the work of Marvila T.M, et al (2021) in which metakaolin was used as an aluminosilicate in the synthesis of activated alkali materials [22]. The presence of these amorphous aluminosilicates is extremely important during the production of the geopolymers due to their high dissolution rate in the highly alkaline environment.

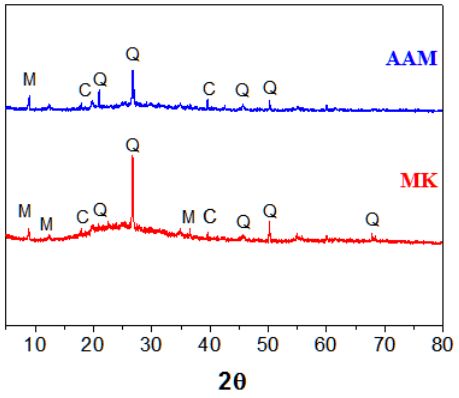

Figure 2. X-ray diffraction of the MK and the AAM formed after 28 days of curing. Q - Quartz (SiO_2), M - Muscovite ($KAl_2Si_3AlO_{10}(OH, F)_2$), C - Kaolinite ($Al_2Si_2O_5(OH)_4$).

In the AAM diffractogram, it is possible to observe that crystalline phases that were present in the MK and that persist after alkali-activation, mainly quartz and kaolinite. This result reinforces the idea that crystalline species do not contribute (or contribute very little) to the dissolution process and the consequent release of Si and Al for the formation of polymeric chains. A similar halo is also observed in the AAM sample, however slightly shifted to higher 2Θ angles, between ~22 and 40°. This displacement is characteristic of the alkaline-activation process and occurred in the sample demonstrating the occurrence of the formation of a matrix with cementitious properties (AAM) [23].

3.2 Infrared spectroscopy

Figure 3 shows the infrared absorption spectra of MK and alkali-activated material after 28 days of curing. It is possible to observe bands at wavelengths close to 3460 and 1660 cm^{-1} that are related to water molecules that are weakly adsorbed on the surface of the MK. Such bands show an increase in intensity after contact with the activating solution, as observed in the AAM spectrum. In the MK spectrum, the band close to 1080 cm^{-1} is attributed to the stretching of the Si-O-Si groups present in the material structure. After contact with the activating solution, these bands move to wavelengths close to 1000 cm^{-1}. This displacement was attributed to the replacement of Si atoms by Al atoms in the structure of the inorganic polymer, forming, at the end of the polycondensation reactions, structures of the Al-O-Si type. This substitution promoted a decrease in the length and angle of the chemical bond after the replacement of silicon atoms in Si-O-Si structures by aluminum, forming Si-O-Al structures in which Si can occupy sites of the type Q^3 or Q^4 [24-26]. Bands close to 540 cm^{-1} and 470 cm^{-1} are bands related to the vibration of Si-O-Al and Si-O-Si, and they tend to appear both in the precursor material and in the gel formed after activation. The bands around 730 cm^{-1} and 697 cm^{-1}, refer to aluminum ring structures and are compared with the phases of zeolites that are formed. It is possible to identify bands close to 1429 cm^{-1} attributed to sodium carbonate, and the crystallization of $Na_3H(CO_3)_2.2H_2O$ may occur as an efflorescence in inorganic polymers [27]. In the studied system, the formation of sodium carbonate can be related by the reaction of excess sodium hydroxide with atmospheric carbon dioxide according to Equation 1:

$$2\ NaOH + CO_2 \rightarrow Na_2CO_3 + H_2O \qquad (1)$$

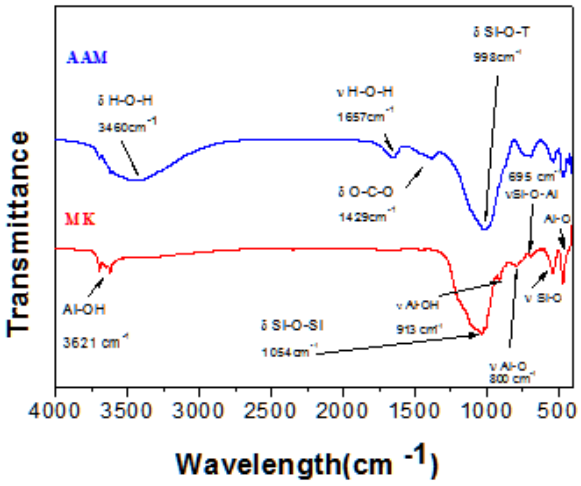

Figure 3. Infrared spectroscopy of the MK and the AAM formed after 28 days of curing.

3.3 Apparent porosity and water absorption

The results for the analysis of the apparent porosity and water absorption of the different samples produced are presented in Figure 4. It is possible to observe that the samples without the addition of EPS (ref.) presented average values close to 40% porosity and 30% for water absorption. The addition of polystyrene decreased the total apparent porosity and it was observed that the increase in the diameter

of the dispersed phase promoted a more pronounced decrease in the porosity of the specimens. The samples containing 18% EPS with 0.85 mm in diameter showed a porosity of 37%, very close to the values presented by the reference sample. However, adding the volumetric percentage values of 53% (sample 53A) resulted in a porosity close to 27% for samples cured at the same time. Such a decrease represents a value of close to 27%. The results obtained for the specimens produced with 2.16 mm EPS beads presented values very close to the results of samples containing 0.85 mm. The samples produced by the insertion of 18-vol% EPS 2.16mm (18B) showed values close to 36% of apparent porosity. The porosity of this material decreased after adding 53% EPS, resulting in values close to 26.6% porosity and showing a decrease close to 26.1%.

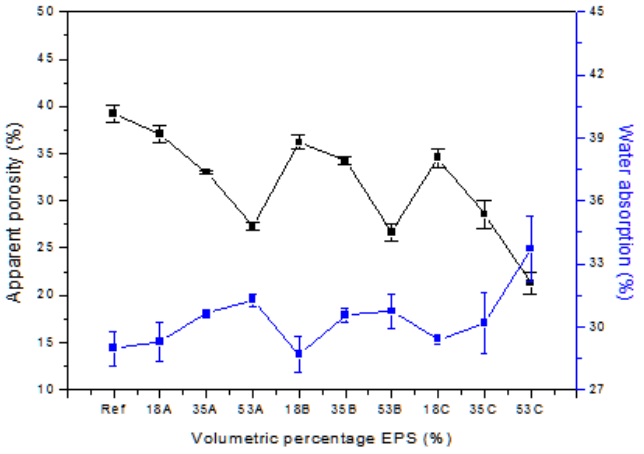

Figure 4. Apparent porosity and water absorption of the reference material and AAC formed after 28 days of curing.

The decrease in the total porosity of the specimens was more pronounced when the diameter of the EPS used was 6.00 mm. Samples containing 18-vol% showed values close to 34.5% and samples 53C (53-vol% - 6.00mm) showed values close to 22.2% and showed a decrease of 35.6% in the total porosity value, the greatest decrease presented between all experimental conditions.

In all samples, it was observed that the increase in the volumetric fraction of EPS promoted a decrease in total apparent porosity. The increase in the volumetric fraction of EPS promotes a decrease in the fraction of the inorganic matrix (AAM), mainly responsible for the porosity of the material. However, the increase in water absorption values was increased when the apparent porosity decreased (an increase of EPS beads percentage). This may be related to the appearance of greater interfaces between the matrix and the dispersed phase that promotes the increase of voids that maximize water absorption. Concomitantly, the increase in the average diameter of the EPS beads favors the appearance of microcracks that are responsible for the increase in the total water absorption of the specimens, as observed in sample C9.

3.4 Apparent density

The results for the analysis of the apparent density of the different samples produced are presented in Figure 5. It is possible to observe that the sample reference presented average values close to 2.23 g/cm^3 of density. The addition of polystyrene decreased the apparent density values and it was observed that the increase in the diameter of the dispersed phase promoted a more pronounced decrease in the density of the specimens. The C1 samples showed average density values close to 1.96 g/cm^3 and decreased to 1.21 g/cm^3 after the addition of 53-vol% EPS. The C4 samples showed an average value of 1.96 (similar to those presented by the C1 samples), which decreased to 1.27 g/cm^3 in the C6 samples (53-vol% - EPS 2.16 mm). In samples C7, C8, and C9, samples produced with the fraction of EPS with a larger diameter, the decrease in density was greater. Values close to 1.86, 1.27, and 0.80 g/cm^3 were obtained for samples C7, C8, and C9, respectively. Such a decrease was close to 38.3, 35.2, and 57%, when different diameters of EPS beads were used, 0.85, 2.16, and 6.00 mm, respectively. The decreases in densities values were associated with the presence of EPS fractions that have a lower density than the matrix produced by alkali-activation of metakaolin. On the other hand, the change in the diameter of the EPS beads is linked to the insertion of particles with lower density values (see Table 4). Thus, the presence of EPS C beads (6.00 mm in diameter) and the subsequent increase in their fraction (C7 - C9) promoted a greater decrease in density values than those observed in composites manufactured with EPS A and B as dispersed phases.

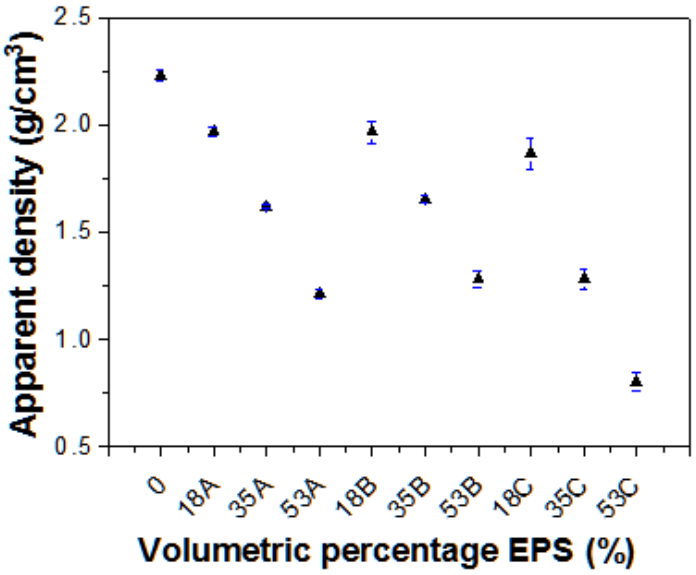

Figure 5. Apparent density of the reference material and AAC formed after 28 days of curing

3.5 Specific mass of the alkali-activated composites

Volumetric density (specific mass) is one of the parameters that control many physical properties in lightweight composites and is mainly influenced by the amount and density of the type of aggregate present in the matrix. Increasing volume percentages of EPS in the AAC promotes a reduction of the volumetric density, as can be observed in Figure 6. The most pronounced difference in the average density occurs for EPS beads with a 6.0 mm diameter (C7 to C9 samples). These results are following previous studies by Babu et al. [28], Babu et al. [29], Chen and Liu [30], Kan and Demirborga [31], and Miled et al. [15], who investigated the addition of EPS as aggregate in concrete mixtures and showed that volumetric density of the composite decreases with increasing EPS volume percentage. When the specimens were produced by the addition of 53-vol% EPS, the average values of the volumetric density were below 1.0 g/cm^3 (water density) demonstrating that they were able to float and still preserve the mechanical integrity of the same. When the AAC was produced with EPS C as a dispersed phase, values below 1.0 g/cm^3 were obtained for samples containing 37-vol%, due to the lower density value presented by EPS beads.

3.6 Microstructure (SEM Analysis)

The longitudinal images of the specimens and SEM images of the reference specimen and AAC surfaces are shown in Figures 7 to 12. Figure 7 presents the longitudinal surface of the reference material has a homogeneous structure, without the presence of many pores and superficial cracks. SEM images showed the formation of a structure of a densified cementing material with few unreacted metakaolin particles, demonstrating the effectiveness of the alkaline solution in dissolving the starting material and forming an inorganic binder structure.

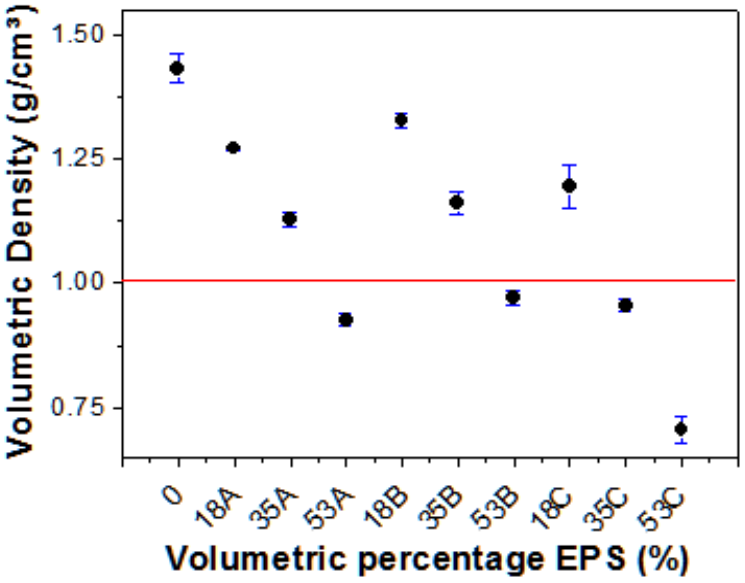

Figure 6. Volumetric density of the reference material and AAC formed after 28 days of curing.

It is possible to observe that the unreacted particles of MK are embedded in the aluminosilicate gel formed. The images of C1 specimens showed the presence of a cementitious matrix similar to that found in the reference material. The presence of unreacted MK particles and embedded in the gel are observed. The EPS beads are embedded in the matrix formed and some regions occupied by the dispersed phase are empty, which may be related to the low adhesion of some EPS particles with the alkali-activated matrix. The SEM images (500 X) indicate that there is very good adhesion between EPS particles and the matrix. EPS particles are completely embedded in the alkali-activated matrix.

The images of sample C4 show similar morphology to that found in sample C1. A dense matrix with few pores and the presence of EPS beads embedded in the gel. It is possible to observe a small amount of material on the EPS beads, which may be related to MK particles and or small fragments of the formed gel. This may be associated with the hydrophobic nature of EPS. The increase in the diameter of EPS beads in samples C7, C8, and C9 modified the morphology of the specimens. It is possible to observe that the dispersed phase did not adhere very well to the inorganic matrix, which caused an interface with voids. With the increase in the volumetric fraction of EPS beads in the composite, it is possible to observe a greater fragmentation of the specimen used for the longitudinal cut. Such fragmentation of the specimen may be associated with a more fragile structure, due to the greater amount of voids caused by the matrix/dispersed phase (EPS) interfaces. It is possible to observe the formation of cracks around the dispersed phase. This fact may be associated with a greater area of stress generation during the hardening of the alkali-activated matrix, which promotes the formation of regions with poor mechanical strength.

3.7 Compressive strength

The compressive strengths of the 28-day cured composites and the reference are shown in Figure 13. Increasing amounts of EPS beads added to the alkali-activated matrix caused a reduction of the mechanical strength, from about 47.5 MPa of the original alkali-activated material (Ref) to 25 MPa when 18 vol.-% (average diameter of 0.85 mm) of EPS was added.

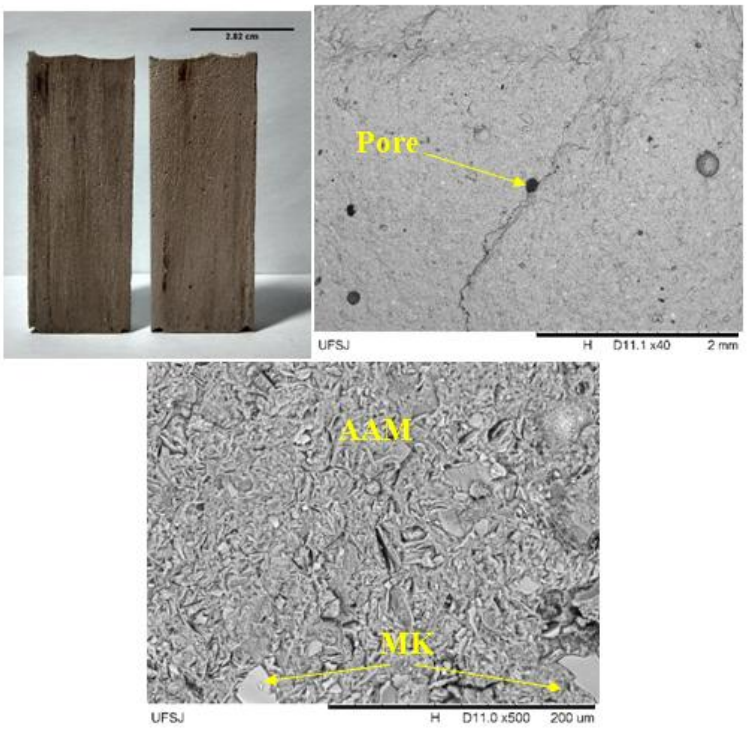

Figure 7. SEM images of the ref AAM sample after 28 days of curing.

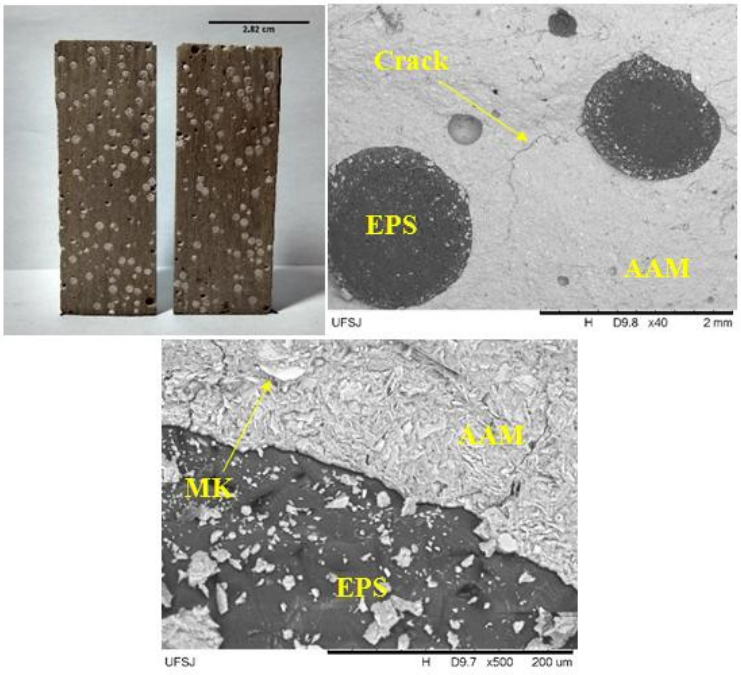

Figure 8. SEM images of the AAC sample (C1) after 28 days of curing.

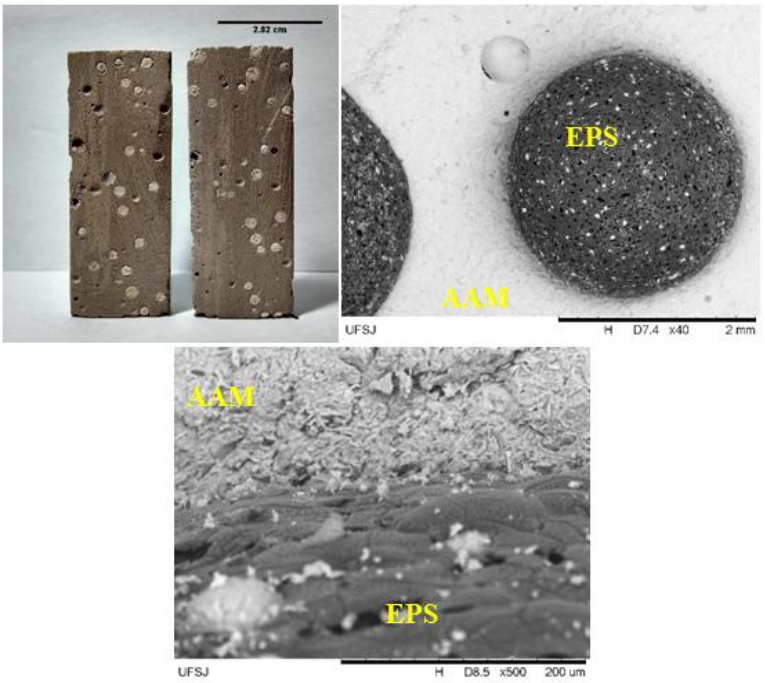

Figure 9. SEM images of the AAC sample (C4) after 28 days of curing.

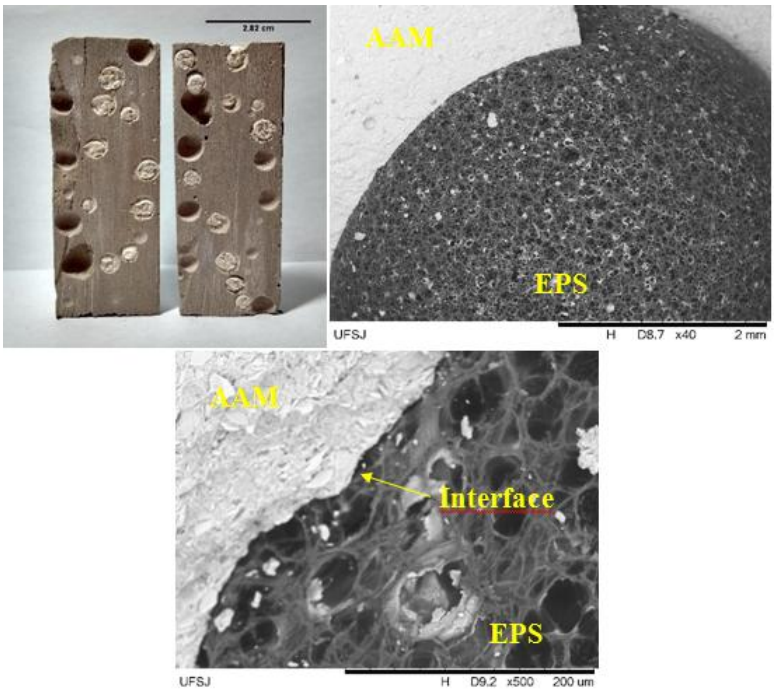

Figure 10. SEM images of the AAC sample (C7) after 28 days of curing.

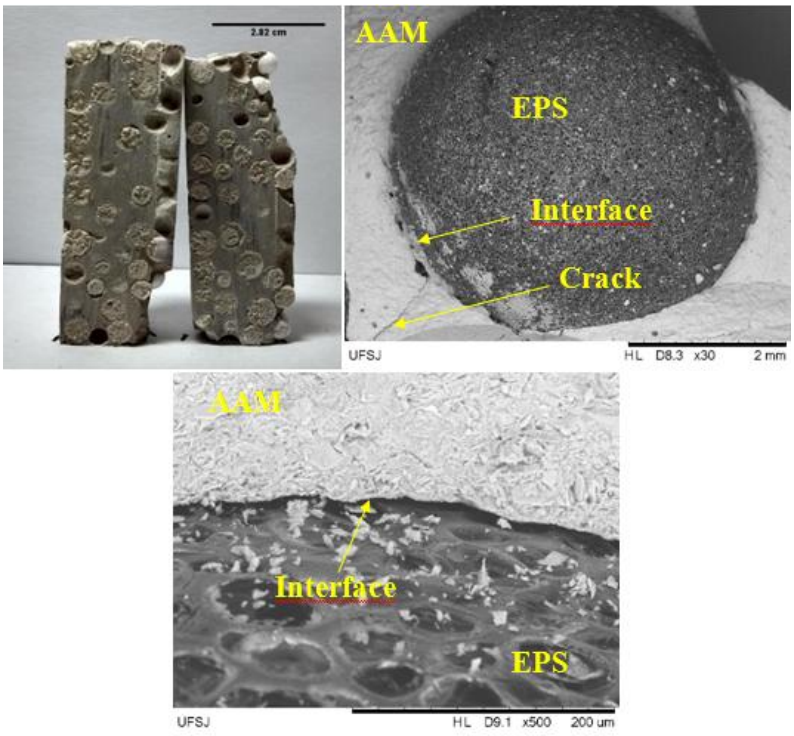

Figure 11. SEM images of the AAC sample (C8) after 28 days of curing.

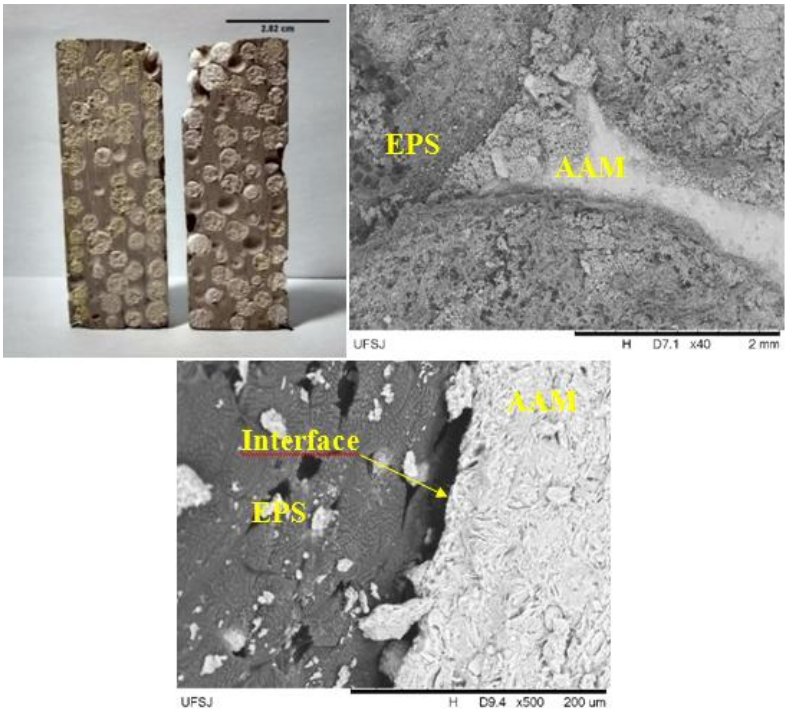

Figure 12. SEM images of the AAC sample (C9) after 28 days of curing.

On the other hand, when 53 vol.-% of EPS beads were added to the system the compressive strength was close to 14 MPa, represent a decrease close to 70% in the mechanical strength of the specimens. Furthermore, it can be observed that the strength decrease is more pronounced for larger EPS beads, i.e. strength decreased to 12.2 MPa and 1.5 MPa when 18 or 53 vol.-% of EPS beads with an average diameter of 6 mm were added. Such a decrease in the mechanical resistance of the specimens represents a decrease close to 88%. These results are in agreement with recent studies conducted by Colangelo et al. [32], who produced alkali-activated composites based on metakaolin, with the incorporation of recycled EPS particles as a dispersed phase with an approximate size of 0.4 to 0.6 mm. The authors report a compressive strength of 3.4 MPa and 1.8 MPa for volumetric percentages of EPS of 65 and 72.5%, respectively.

These results are similar a very few articles on the incorporation of EPS in an alkali-activated matrix have been published; more work has been done with Portland cement – the so-called EPS concrete. Babu et al. [31], investigated the addition of EPS beads with average diameters of 4.75 and 6.3 mm varying its contents between 21 and 36 vol.-%. The strength of EPS concrete increased with a decrease in the EPS bead size for the same mix proportions, from 15.0 MPa to 10.2 MPa, and from 19.8 MPa to 10.2 MPa when using smaller beads compared to larger beads and contents of 33.2 and 22.2 vol-%.

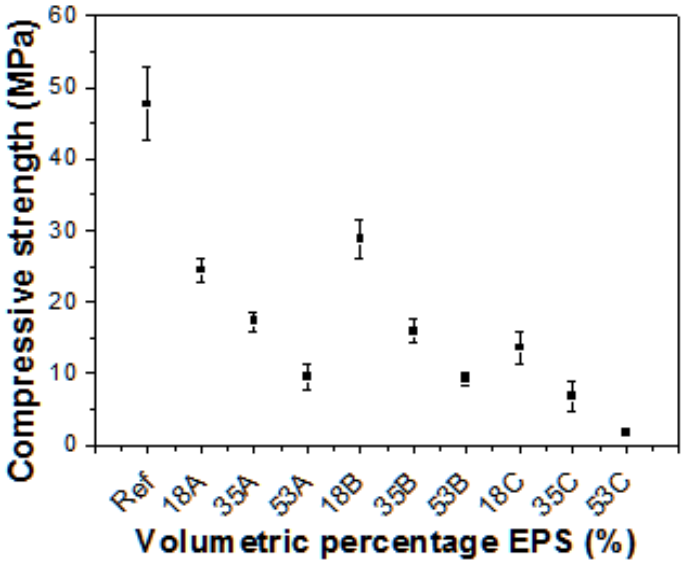

Figure 13. Compressive strength of Ref and samples C1 to C9 after 28 days of curing.

The decrease in the compressive strength values of the composites may be associated with the decrease in the density of the specimens with the increase in the volumetric fraction of EPS and the diameters of EPS beads. The relation between the decreased density of specimens and decreased compressive strength of AAC (specific strength) can be seen in Figure 14. The decrease in density, related to the increase in the volumetric percentage of EPS promotes the achievement of AAC with lower values of resistance to comprehension. Increasing the volumetric percentage of EPS in the samples produced decreases the mechanical strength of the samples. Such changes prevent the material from being used in structural applications (where high strength is required). As observed by SEM analysis, the increase in the volumetric fraction promoted an increase in the number of matrix/EPS interfaces

that accumulate stresses and may be related for the formation of microcracks and avoids that decrease the resistance of the specimens. Furthermore, it was observed by the images that the insertion of EPS beads with larger diameters promoted a decrease in adhesion between the alkali-activated matrix and the EPS particles. This fact may be related to the poor results of the compressive strength of these materials.

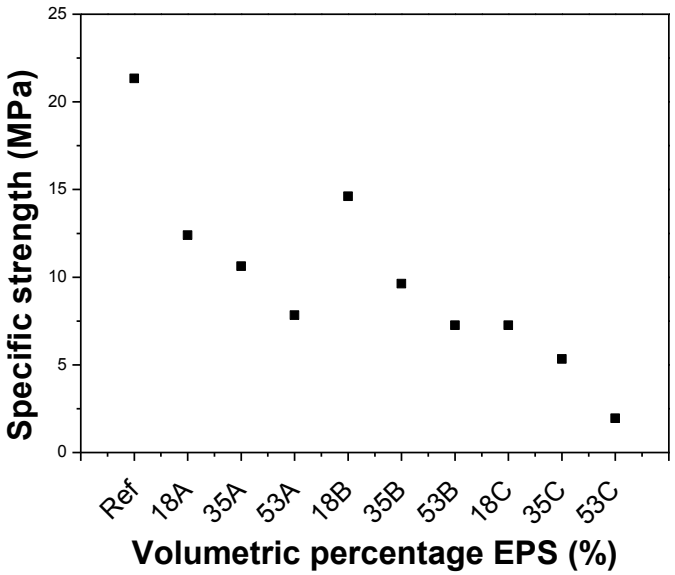

Figure 14. Specific strength of the reference specimens and AAC after 28 days of curing.

4. CONCLUSIONS

The alkali-activated composites produced from the alkaline activation of MK with sodium hydroxide solution and sodium silicate, together with EPS beads as aggregate, presented physical and mechanical properties that favor their use in some areas of civil construction because of their low density and reasonable mechanical strength. Increasing amounts of EPS in the composites significantly altered the compressive strength of the specimens. Addicting EPS as aggregate to the alkali-activated low-density composites (0.8-1.2g/cm³) could be obtained. This decrease in the composite´s density is an important property to be controlled for its subsequent use. The decrease in density due to the increase in EPS volume makes the material lose some structural applications but favors its use as a thermal and acoustic coating. The increase in the amount of EPS in composites favors a material with high amounts of voids which increase the effectiveness of the properties mentioned as possible applications. Microstructural investigations revealed that the addition of EPS did not interfere with the formation of the inorganic aluminosilicate gel, and the presence of non-reacted MK particles embedded in the aluminosilicate gel was irrelevant in the process. However, its application in the industry, both in construction and in other areas, should be treated with caution due to the physical properties of these composites, requiring further investigation.

5. ACKNOWLEDGMENT

This work was developed with the support of the financing agency, CAPES: Coordenação de Aperfeiçoamento de Pessoal de Nível Superior and Universidade Federal de São João del-Rei (UFSJ).

6. REFERENCES

[1]. Huiskes DMA, Kwhen A, Yu QL, Brouwers HJH. Mater. Des. 2016; 89 (10): 516-526.

[2]. Wianglor K, Sinthupinyo S, Piyaworopaiboou M, Chaipanich, A. Appl. Clay. Sci. 2017; 141 (7): 272-279.

[3]. Rovnaník P. Constr. Build. Mater. 2010; 24 (7): 1176-1183.

[4]. Bing-hui M, Zhu H, Xue-Min C, Yan H, Si-Yu G. Appl. Clay. Sci. 2014; 99 (4): p. 144-148.

[5]. Zhang M, Zhao M, Zhang G, El-Korchin T, Tao M. Cem. Concr. Compos. 2017; 78 (11): 21-32.

[6]. Palomo A, Maltseva O, Garcia-Lodeiro I, Fernández-Jiménez A. Front. Chem. 2021; 9: 653.

[7]. Provis JL, Bernal SA. Mater. Res. 2014; 44 (18): 299-327.

[8]. Barroso MDB. Tese de doutorado. 2009: 1-64.

[9]. Palomo A, Grutzeck MW, Blanco MT. Cem. Concr. Res. 1999; 29 (7): 1323-1329.

[10]. Azevedo ARG, Marvila MT, Reis L, Carlos C, Fontes M. Int. J. Appl. Ceram. Technol. 2020; 17 (9): 2649–2658.

[11]. Marvila MT, Azevedo ARG, Barbosa L, Oliveira D, Castro G, Maurício C, Vieira F. Case. Stud. Constr. Mater. 2021; 15: e00723.

[12]. Davidovits R, James C. Int. Conf. 1999: 1-8.

[13]. Kan A, Demirboga R. Cem. Concr. Res. 2009; 31 (6): 489-495.

[14]. Ganesh Babu K, Saradhi Babu D. Cem. Concr. Res. 2003; 33 (7): 755-762.

[15]. Miled K, Le Roy R, Sab K, Boulay C. Mech. Mater. 2004; 36 (15): 1031-1046.

[16]. Dueramae S, Sanboonsiri S, Suntadyon T, Aoudta B, Tangchirapat W, Jongpradist P, Pulngern T, Jitsangiam P, Jaturapitakkul C. Constr. Build. Mater. 2021; 297: 123769.

[17]. Azevedo ARG, Marvila MT, Ali M, Khan MI, Masood F, Vieira CMF, Case. Stud. Constr. Mater. 2021; 15: e00662.

[18]. Montgomery DC. John Wiley & Sons. 1997: 1-108.

[19]. Werkema MCC, Aguiar S. Escola de Engenharia da UFMG. 1996.

[20]. ABNT NBR 5739. Norma Brasileira. 2018; 3ed: 1-13.

[21]. BS EN ISO 10545-3. Ceram. Tiles. 1997; 1ed: 1-10.

[22]. Marvila MT, Azevedo ARG, Delaqua GCG, Mendes BC, Pedroti LG, Vieira CMF. Constr. Build. Mater. 2021; 286: 122994.

[23]. Tambara Júnior LUD, Cheriaf M, Rocha JC. Compos. Mater. 2018; 11 (22): 1-22.

[24]. Azevedo AGS, Strecker K, Lombardi CT. Cerâmica. 2018; 64 (10): 388-398.

[25]. Li W, Lemougna PN, Wang K, He Y, Tong Z, Cui X. Ceram. Int. 2017; 43 (6): 14340-14346.

[26]. He P, Wang M, Fhu S, Jia D, Yan S, Yuan J, Xu J, Wang P, Zhou Y. Ceram. Int. 2016; 42 (6): 14416-14422.

[27]. Azevedo AGS, Strecker K. Ceram. Int. 2017; 43 (7): 9012-9018.

[28]. Babu GK, Babu SD. Cem. Concr. Res. 2003. 33

(7): 755-762.

[29]. Babu GK, Babu SD. Cem. Concr. Compos. 2004; 26 (6): 605-611.

[30]. Liu N, Chen B. Constr. Build. Mater. 2014; 68 (5): 227-232.

[31]. Kan A, Demirborga R. J. Eng. Sci. Mater. Sci. 2007. 14 (2): 158-162.

[32]. Colangelo F, Roviello G, Ricciotti L, Ferrandiz-Mas V, Messina F, Ferone C, Tarallo O, Cioffi R, Cheeseman CR. Cem. Concr. Compos 2016. 86 (6): 266-272.

7. MINIBIOGRAFÍA DE AUTORES

Adriano Galvão de Souza Azevedo is currently researcher at São Paulo University (USP) - FZEA-Pirassununga/SP. Ph.D. in Physics and Chemistry of Materials (2017). Master in Physics and Chemistry of Materials (2013). Is Graduated in Chemistry (2011) and works with the production of clinker-free inorganic binders. https://orcid.org/0000-0002-8811-9879

Luis Fernando Tonholo Domingos is currently doctoral student at the Federal University of São João Del-Rei (UFSJ). Master in Physics and Chemistry of Materials (2018). Is Graduated in Chemistry (2016) and works with the production of clinker-free inorganic binders. https://orcid.org/0000-0003-2605-1220

Carolina Torga Lombardi is graduated in Mechanical Engineering from the Federal University of São João Del-Rei (2016) and Master in Mechanical Engineering from the Federal University of São João Del-Rei (2019), working mainly on the following topics: geopolymer composites and geopolymerization using metakaolin as raw material.

Kurt Strecker is Graduated in Materials Science - Universitat Erlangen-Nurnberg (Friedrich-Alexander) (1986) and Ph.D. in Materials Engineering - Max Planck Institute, Stuttgart (1990), recognized by UFSCar. He held a Postdoctoral degree (2001) at the Universität Karlsruhe, Germany, and is a Professor at the Escola Politécnica da USP (2006). He is currently Full Professor at the Federal University of São João del-Rei. He has experience in Materials and Metallurgical Engineering, with an emphasis on Ceramics (advanced and traditional), working mainly on the following topics: sintering, microstructure and mechanical properties. Currently develops works of composite materials using industrial and residential waste. He has experience in leading international cooperation projects (Max-Planck Institut-Germany, Universität Karlsruhe-Germany, University of Aveiro-Portugal, Universidad Eduardo Mondlane-Mozambique). https://orcid.org/0000-0001-6164-7906.